Spatio-temporal effect of urban heat island on cardiovascular diseases

Huanchun Huang (huangyanlin2010@163.com)
Nanjing Forestry University https://orcid.org/0000-0002-3330-3732
Deng Xin
nanjling forestry university
Yang Hailin
nanjing foresry university
Hao Cui
Peking University People's Hospital
Peng Zhongren
University of Florida
Liu Wei
nanjing forestry university

Research article

Keywords: Urban heat island, cardiovascular disease, landscape pattern, spatio-temporal feature

Posted Date: November 14th, 2019

DOI: https://doi.org/10.21203/rs.2.17316/v1

RESEARCH ARTICLE

Spatio-temporal effect of urban heat island on cardiovascular diseases

Authors

Huang Huanchun[1], Deng Xin[1], Yang Hailin[1], Hao Cui[2], Peng Zhongren[3], Liu Wei[1]

Institutional Affiliations

[1]School of Landscape Architecture, Nanjing Forestry University, Nanjing, China, 210037

[2]Beijing Meteorological Station, Beijing, China, 100089

[3]College of Design, Construction and Planning, University of Florida, Gainesville, USA, 210036

Corresponding author

Huang Huanchun,

[1]School of Landscape Architecture, Nanjing Forestry University, China

E-mail addresses: huangyanlin2010@163.com(Huang Huanchun); 1033052652@qq.com (Deng Xin); 1075746209@qq.com (Yang Hailin); 754655876@qq.com (Hao Cui); 36259471@qq.com (Liu Wei)

Abstract

Background: As urbanization progresses, urban built-up areas are expanding, increasing the number of urban heat islands (UHIs) and damaging the cardiovascular health of urban residents. This study aimed to explore the spatio-temporal pattern evolution characteristics of the effect of UHI on cardiovascular diseases (CVDs).

Methods: We analyzed the land surface temperatures (LSTs) retrieved from data from four Landsat remote-sensing images from 1984 to 2017, data on temperature from 95 meteorological stations, and data on CVDs mortality. Based on this, landscape pattern indices were used to analyze the pattern-process-function underlying the effect of UHIs on CVDs.

Results: The effect of UHIs on CVDs increased, thereby increasing the mortality rate by 28.8% and increasing the affected area by 1683.977 km² between 1984 and 2017. The affected areas gradually expanded from the central area of the city, and underwent three evolution stages; the areas highly affected were mainly distributed in the central and southern regions. Patches increased in number, whereas the landscape was fragmented. The area and ratio of high-level patches also showed an upward tendency, increasing the dominance in the overall landscape. The patches of the overall landscape became more complicated in shape, whereas those of high-level ones became less complicated. The degree of concentration of the overall landscape decreased gradually, with the types of landscape patches increasing, reaching a rather even space distribution.

Conclusions: UHIs drastically increase CVDs mortality by increasing temperatures during summer in Beijing, China. As cities expand, the effect of UHIs on CVDs increases in terms of both intensity and area, with overall landscape in uneven distribution, high-level affected areas in point distribution, and low-level ones in large-area concentration. This study, hence, provides theoretical evidence for the prevention and early warning on CVDs.

Keywords

Urban heat island, cardiovascular disease, landscape pattern, spatio-temporal feature

Background

Currently, 50% of the world's population lives in cities, and this proportion is expected to rise to 68% by 2050 [1]. As a result, people migrate into cities, and the built-up area continues to expand, which makes the temperature in urban areas significantly higher than that in the surrounding rural areas [2]. It, thus, severely affects the health of urban residents, especially in terms of the cardiovascular system.

Cardiovascular diseases (CVDs), such as coronary heart disease, cerebrovascular disease, peripheral vascular disease, rheumatic heart disease, congenital heart disease, and heart failure, are disorders of the heart and blood vessels. CVDs are the leading cause of death worldwide. In 2016, a total of 17.9 million people died from CVDs, accounting for 31% of all deaths worldwide. CVDs and their associated deaths are caused by a number of factors [3]. As a result, many epidemiological studies have explored the relationship between air temperature and CVDs [4].

The excess mortality that occurs during summers is usually attributed to an increased prevalence of CVDs [5,6]. The relationship between temperature and mortality due to CVDs is usually depicted as U-, V-, or J-shaped, indicating that the mortality rate increases gradually when temperature exceeds the threshold [7]. Threshold temperature, a critical standard for identifying the extent of urban heat island (UHI) damage on health [8], can help explore the spatio-temporal pattern of the effect of UHI on CVDs. studies have revealed threshold temperatures. Previous studies, however, mainly focused on quantifying the epidemiologic effect of environmental temperature on CVDs, which was unable to explain the mechanism

71 underlying the spatio-temporal interaction between them.

72 Recently, some scholars have used landscape pattern indices to analyze the
73 spatio-temporal evolution of heat island landscapes [9,10], but not the effect of the
74 spatio-temporal response mechanism of UHI on human health. In addition, the
75 landscape pattern is related to multiple diseases [11,12]. study proved that a positive
76 correlation exists between regional landscape fragmentation and temperature and the
77 incidence rate of Lyme disease [13]. These indicate that the landscape pattern is
78 related to human health, but the focus is always on landscape patterns and the
79 mechanisms by which landscape structures affect disease, and not exploring
80 landscape-pattern-process of the effect of UHI on human health. Thus, this study used
81 the landscape pattern index to study the spatio-temporal evolution of the effect of UHI
82 on CVDs and reveal the pattern-process-function and influencing mechanism of UHI
83 on CVDs.

84 From 1984 to 2018, the UHI effect has become more serious, and the incidence
85 of heat wave has increased significantly, particularly in world-class mega-cities like
86 Beijing. This has led to a sharp increase in mortality due to CVDs. However, the
87 effects of spatio-temporal characteristics of UHI on CVDs mortality remain unclear.
88 This study used data from Landsat remote-sensing, meteorological stations, and maps,
89 to analyze the spatio-temporal evolution of the landscape pattern of UHI on CVDs
90 using data analysis software, such as ENVI, ArcGIS, and Fragstats. Ultimately, this
91 study should provide decision-making evidence for healthy urban planning and
92 optimization of ecological environments, thereby reducing the heat exposure risk of

patients with CVDs.

Methods

Data sources and preprocessing

Data sources

Data on temperature were retrieved from Landsat satellite images and meteorological stations. The remote-sensing images were taken on August 16 1984, June 17 1991, August 2 1999, and July 10 2017. When the satellite was present in Chinese territory, atmospheric visibility was sound without cloud covering the study area, and the average wind speed two days before image collection was below 2.3 m/s without any precipitation. The meteorological data were collected via hourly observations from the 96 meteorological stations in Beijing.

CVDs (I00–I60) were classified according to the International Classification of Diseases, 10th revision (ICD-10). Data on CVD mortality in Beijing were obtained from the analysis of the Chinese Center for Disease Control and Prevention [14].

Data preprocessing

First, a radiometric calibration was performed according to NASA's Landsat handbook [15], and digital number values were converted into the corresponding thermal radiation intensity L(λ) values. The images were calibrated to 0.5 m resolution, and any error was controlled within 1 pixel. Next, data were resampled to 30 m resolution to be projected to the WGS_1984_UTM_50N coordination system.

Last, a database was established using the ArcGIS software to extract remote-sensing data in different periods for analysis.

Research methods

Air temperature retrieval

Land surface temperature (LST) and near-surface air temperature (NSAT) are two important parameters for studying the interaction mechanisms of UHI; a good correlation can be established between both. Concurrently, studies prove that LST and land surface index by Thematic Mapper (TM) retrieved [16] can serve as valid data to study urban thermal health [17].

Atmospheric calibration was applied in this study. First, radiometric calibration was performed according to the NASA manual (landsat.usgs.gov/documents) to transform the digital number into relevant heat radiation intensity. Then, the normalized difference vegetation index (NDVI) and vegetation coverage were calculated. Next, the calculation method for emissivity proposed by Qin et al. was used to obtain land surface emissivity via NDVI and vegetation coverage [18]. Finally, LST was calculated using the following (T_L) formula:

$$T_L = \frac{T}{1+(\lambda T/\rho)\ln\varepsilon} \quad 273.15 \qquad (1)$$

where λ is the central wavelength of TM6 band (11.5 μm), $\rho = h \times \frac{c}{\sigma} = 1.438 \times 10^{-2} K$ (where Stefan-Boltzmann's constant $\sigma = 1.38 \times 10^{-23} J/K$, Planck's constant $h = 6.626 \times 10^{-34} Js$, and speed of light,

136 $c = 2.998 \times \frac{10^8 m}{s}$).

137 Data on LST retrieval were collected from the tests in 95 surface meteorological
138 stations between July 10 and August 22 2015, based on which the temperature
139 regression formula was established. The regression formula of land surface
140 temperature was established by using the land surface temperature inversion data of
141 95 weather stations from July 10 to August 22, 2015. These 95 surface meteorological
142 stations are prioritized from 360 surface meteorological stations. First, the coefficient
143 among NDVI, normalized difference water index (NDWI), architectural composition,
144 and daily average temperature were calculated in various scales. The results revealed
145 that daily average temperature was closely related to NDVI at 160 m and LST at 300
146 m resolution. Next, software, such as SPSS and MATLAB, were used for curvilinear
147 regression, indicating that sound regression results had a linear polynomial
148 relationship, and that regression formulas enhance the robustness of sound. The
149 coefficient of determination (R^2) was 0.95, the root-mean-square error was 0.13, and
150 the regression formula was as follows:

151 $$T_A = 4.31 + 0.1679 T_L - 0.1747 y \quad (2)$$

152 where T_A is the daily average temperature, T_L is the LST, and y is the NDVI.

153

154 Relationship between increased UHI and increasing CVD mortality

155 UHI controls urban temperature, which leads to increased morbidity and mortality
156 rates due to CVDs, but the effect of high temperature on such mortality still faces a
157 key threshold [19,20]. Based on daily temperature and CVD mortality data from 2007

158 to 2013 in Jinan, China, Li estimated the thermal threshold of CVD mortality using
159 observation and prospective analysis. The results showed that the maximum, average,
160 and minimum threshold temperatures in Jinan were 32°C, 28°C, and 24°C, with 4.1%,
161 7.2%, and 6.6% increases in mortality rates, respectively, per unit rise in temperature
162 [14] (Fig. 1). This is because Beijing and Jinan belong to the temperate monsoon and
163 the difference in longitude is small. They both belong to megacities on the same
164 longitude. Therefore, based on the relationship between daily mean temperature and
165 CVD mortality assessed, this study explores the spatio-temporal evolution of the
166 effect of UHI on CVDs.
167

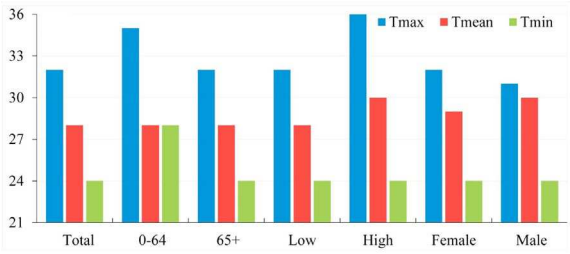

168
169 Fig. 1. Heat thresholds of Tmax/Tmean/Tmin [14]

170 Grading of the effect of UHI on CVDs

171 Modern medical studies have revealed that environmental temperature is closely
172 related to the physiological activities of the human body. The coziest environmental
173 temperature is 20–28°C. When the body temperature exceeds 28°C, our blood vessels
174 dilate, transporting more blood to the skin surface, thereby increasing the temperature
175 of the skin and making us feel uncomfortable. Once the temperature exceeds 30°C,
176 some sweat glands are activated to dissipate heat in the form of perspiration, thereby
177 dilating the skin vessels and re-allocating the blood. Concurrently, more blood enters

and leaves the heart, increasing the cardiac load [21,22]. When the temperature increases beyond 32 °C, it reaches the maximum threshold temperature for CVD mortality in Jinan [14].

All in all, according to the threshold temperature and the physiological response of the human body to high temperature, this study was based on the threshold temperature at which UHI affected CVDs in Beijing with the daily average temperature of 28°C, and the UHI intensity was 2°C. With each unit increase in threshold temperature, the mortality rate increased by 7.2%. Therefore, we classified the effect of UHI on CVD mortality into five levels as shown in Table 1. Level 1 implied that UHI had a lower effect on CVD mortality. Levels 2, 3, 4, and 5 represent medium, high, and very high effects.

Table 1. Grading of the effect of UHI on CVDs mortality

Level	Temperature (℃)	UHI intensity (°C)	Increase in mortality rate (%)	Remark
Level 1	28–29	2.7–3.7	0–7.2	Humans starts to feel a little uncomfortable
Level 2	29–30	3.7–4.7	7.2–14.4	Humans feel uncomfortable, with slight sweating
Level 3	30–31	4.7–5.7	14.4–21.6	Humans feel very uncomfortable, with much sweating
Level 4	31–32	5.7–6.7	21.6–28.8	Cardiovascular system starts to be affected, with increased cardiac output, aggravated cardiac load
Level 5	32+	6.7+	28.8–36	Temperature reaches the critical value of daily maximum temperature for CVD mortality

Methods of evaluation of landscape pattern indices

Landscape pattern refers to the permutation of landscape patches of various sizes in the landscape space [23]. Quantitative analysis could be performed on changes and differentiation characteristics of landscape patterns by introducing landscape pattern indices. The indices include three levels: patch, class, and landscape. This study, therefore, started from class and landscape levels and selected 10 landscape pattern indices to quantitatively describe the landscape pattern characteristics that yield an effect on CVDs. The indices selected include class level — PD, cohesion (COHESION), and landscape shape index (LSI); and landscape level — main patch area (AREA_MN), shape index (SHAPE_AM), aggregation index (AI), contagion index (CONTAG), and Shannon diversity index (SHDI) [24]. Indices of the class level demonstrate the quantity and structure of patch types at all levels, whereas those of the landscape level reflect the global feature of the study area.

Survey of Research Areas

Beijing (39.56°N, 116.20°E), one of the first-tier cities in the world, is the center for politics, economy, and culture of China, belonging to the semi-humid continental monsoon of the north temperate zone, which is hot and humid during summer. At the end of 2018, the permanent population in Beijing reached 21.542 million, the rate of urbanization was 86.5%, and the gross domestic product exceeded 3 trillion Yuan.

As the population and economy rocketed, environmental problems, such as UHI arose, yielding a negative impact on both the physiological and psychological health of urban residents. Against the backdrop of economic globalization, the urban sprawl in Beijing became more probable as UHI became more serious [25]; thus, high temperatures engulfed Beijing for 22 days in 2017, gaining worldwide attention. It is therefore of significance to study UHI in Beijing (Fig. 2).

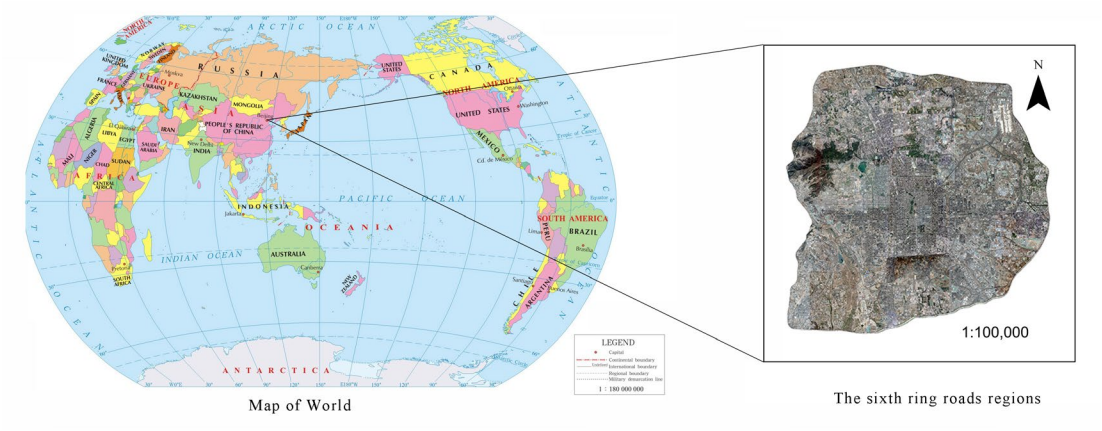

Fig. 2. Outline of the study area

Results

Spatial characteristics of the effect of UHI on CVDs

During 1984–2017, the effect of UHI on CVDs increased from level 2 to level 4, resulting in a 28.8% increase in mortality rate and a 1683.977 km² increase in the affected area. Affected areas showed a trend of expansion from the central area outwards in spatial distribution, showing an obvious spatio-temporal correlation with the process of urban sprawl. The highly affected areas were chiefly concentrated in the central and southern parts; the air temperature in the northern mountainous area was relatively low, making it easier to build up high pressure. Meanwhile, air

temperature in the urban area was relatively high, resulting in low pressure and triggering cold air flow from the northern mountainous area to the urban area.

As illustrated in Fig. 3, levels 1 and 2 affected areas only emerged within the sixth ring road of Beijing during 1984–1999; no highly affected areas were spotted. In detail, level 1 affected areas were mainly distributed in the urban center, gradually expanding to the southern suburbs. Level 2 affected areas were smaller and scattered in the south. In 2017, level 1 patches shrunk drastically, whereas level 2 patches expanded drastically and transformed from scattered points to relatively concentrated plates and facets. Meanwhile, some low-level patches in business centers transformed into high-level patches. Such drastic changes in the spatial distribution of all affected areas were triggered by the fact that in the past two decades, Beijing city (particularly the urban area) developed rapidly as businesses increased, resulting in a series of environmental problems and affecting the cardiovascular health of residents.

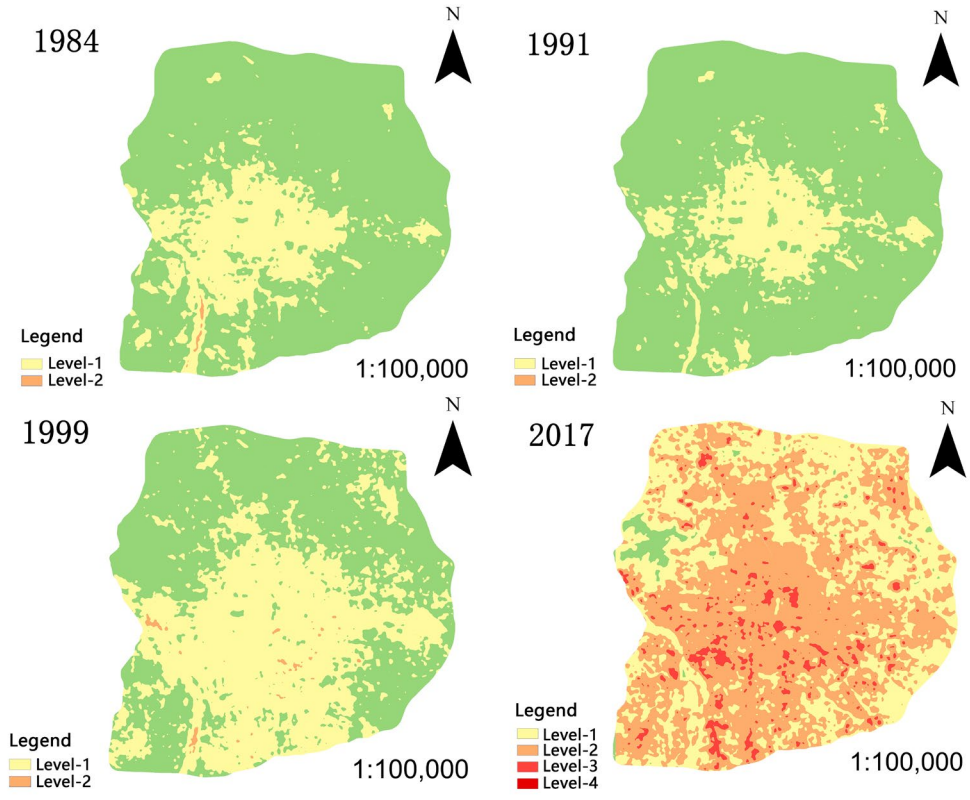

Fig. 3. Distribution of affected areas during 1984–2017

Landscape pattern analysis of the effect of UHI on CVDs

Changes in class level

The changes in PD between 1984 and 2017 are shown in Table 2. In general, PD increased in a fluctuating manner, indicating that affected areas at all levels showed a tremendous trend of fragmentation and separation. In detail, during 1984–1991, levels 1 and 2 affected areas increased slowly yet stably due to the rather slow pace of urban construction. During 1999–2017, however, levels 1 and 2 affected areas decreased, whereas levels 3 and 4 affected areas emerged. This was mainly because urban sprawl tremendously increased the temperature in urban centers, exacerbated the cardiovascular health of residents, and led to a gradual transformation of level 1

affected areas into high-level ones.

Table 2. Changes in PD during 1992–2018

	1984	1991	1999	2017
Level 1	0.0692	0.078	0.1159	0.0957
Level 2	0.0022	0.0022	0.0159	0.071
Level 3	0	0	0	0.1275
Level 4	0	0	0	0.0004

The changes in LSI between 1984 and 2017 are shown in Table 3. LSI increased generally, indicating that affected areas at all levels became more complicated in shape. During 1999–2017, the LSI of levels 1 and 2 affected areas increased rapidly; the fast urbanization triggered the expansion of urban shape and added many patches of independent built-up areas. Meanwhile, levels 3 and 4 affected areas were less complicated because high-level affected areas were mainly concentrated in business centers and resident areas where patch shapes tended to be simpler.

Table 3. Changes in LSI during 1992–2018

	1984	1991	1999	2017
Level 1	12.1617	13.1989	14.5865	23.0332
Level 2	3.5948	2.3	6.8798	22.6149
Level 3	0	0	0	18.6593
Level 4	0	0	0	1.0714

The changes in COHESION between 1984 and 2017 are shown in Table 4. The COHESION of level 1 affected areas was stable, indicating that patches shared sound interconnectivity with relatively concentrated distribution, which was not beneficial to the rapid thermal dissipation inside patches. The elevated air temperature increased the CVD mortality rate. COHESION of level 2 affected areas fluctuated due to urban renovation. In addition, COHESION of levels 3 and 4 affected areas were relatively low with weaker interconnectivity; patches were small in area and distributed in points.

Table 4. Changes in COHESION during 1992–2018

	1984	1991	1999	2017
Level 1	99.8218	99.6738	99.8833	99.7612
Level 2	97.0525	90.0021	96.2389	99.9433
Level 3	0	0	0	96.9449
Level 4	0	0	0	84.978

Changes in landscape level

The changes in PD and AREA_MN between 1984 and 2017 are shown in Fig. 4. PD increased generally, whereas AREA_MN index decreased, indicating that the landscape distribution was heading towards fragmentation. During 1984–1991, PD and AREA_MN nearly remained unchanged due to the rather slow pace of urban construction.

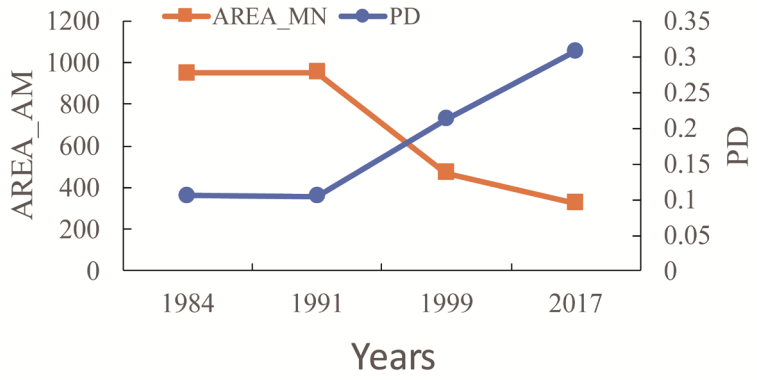

Fig. 4. Changes in PD and AREA_MN during 1984–2017

The changes in SHAPE_AM between 1984 and 2017 are shown in Fig. 5. SHAPE_AM increased generally, indicating that the shape of all affected areas became irregular and that the effect of UHI on CVDs became much more complicated in spatial distribution. During 1984–1999, SHAPE_AM increased steadily due to the rather slow pace of urban development and that urban form was quite stable. However, SHAPE_AM increased rapidly during 1999–2017; rapid urban development and three-dimensional expansion resulted in many new business centers and development projects.

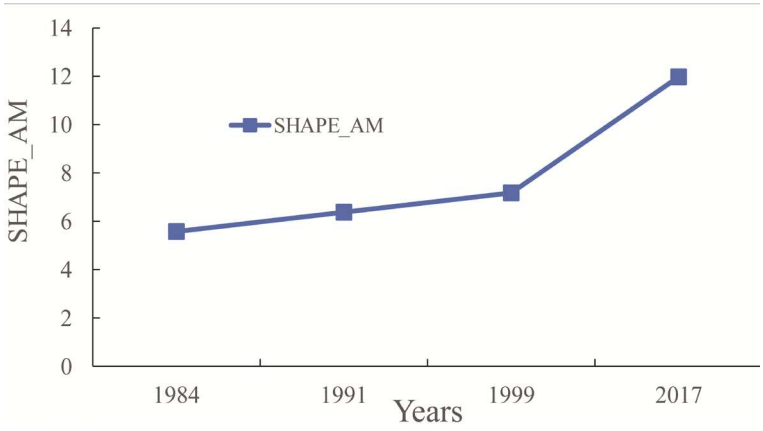

Fig. 5. Changes in SHAPE_AM during 1984–2017

The changes in AI and SHDI between 1984 and 2017 are shown in Fig. 6. AI decreased in general, indicating that the overall landscape was distributed in a scattered manner, and that the landscape was highly fragmented. Patch adjacency was much more decentralized, and the interconnectivity within the affected areas was weak. During 1984–2017, SHDI, an index that describes the diversity of patch, increased generally, indicating that urban built-up areas expanded towards suburbs. In addition, the increased UHI yielded a greater impact on many types of landscape patches with a higher degree of fragmentation. During 1984–1991, SHDI decreased slightly; the effect of UHI on CVD mortality was not very obvious as urbanization slowed down, so that the expansion of level 2 areas dropped in scale, resulting in reduced diversity of patch types.

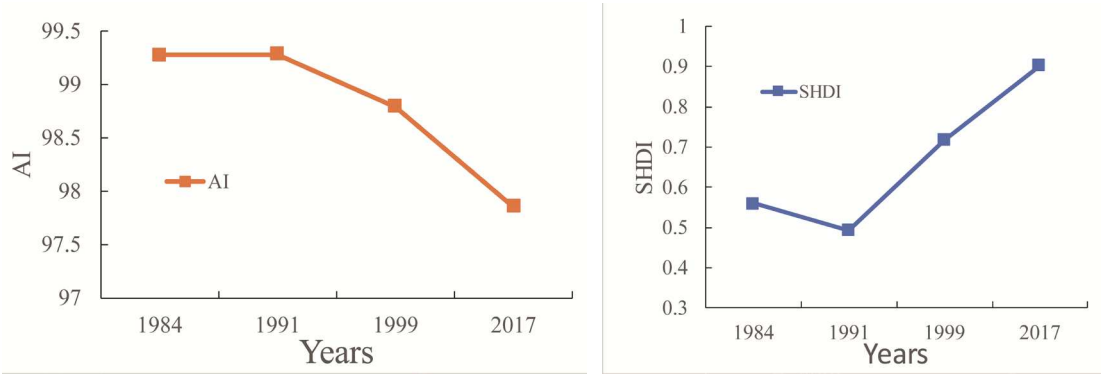

Fig. 6. Changes in AI and SHDI during 1984–2017

Response mechanism of UHI on CVDs

High temperature increases CVD mortality by affecting cardiopulmonary functions, including the blood pressure, blood viscosity, serum cholesterol, and heart rate [26,27]. First, elevated air temperatures increase the heart rate and myocardial oxygen consumption in the human body. Meanwhile blood is transported faster from organs to

318 the skin surface, creating higher pressure on the heart and lungs [28], further
319 increasing the incidence rate of CVDs. In addition, the amount of perspiration from
320 the human body increases. Conversely, this leads to a massive loss of sodium, pH
321 imbalance, and electrolyte disturbance in cells, further resulting in arrhythmia and
322 malfunction of the circulation system, which eventually induces CVDs [29].
323 Conversely, blood viscosity and cholesterol level increase, but the effective
324 circulating volume decreases, triggering insufficient blood supply through the
325 coronary arteries and even myocardial infarction [30]. Last, inappropriate use of air
326 conditioning also indirectly increases the CVD mortality rate. In detail, when the
327 indoor-outdoor temperature difference is >8°C, it becomes difficult for the human
328 body to adjust to the current temperature within a short time. Such drastic differences
329 lead to continuous constriction or dilatation of blood vessels, resulting in a
330 disturbance of blood circulation and further triggering myocardial infarction or stroke.
331 UHI mainly affects CVD mortality among elderly people older than 65 years by
332 increasing temperature during summer. Under high temperatures, the body functions
333 of elderly people decline and the amount and rate of perspiration of each gland
334 reduces; thus, loss of heat in turn increases the accumulated heat inside the body,
335 exacerbating the tension on the cardiovascular system. Under long-term thermal
336 stimulation, constant perspiration causes the blood plasma volume to decrease
337 dramatically; however, blood viscosity increases, thereby increasing the CVD
338 mortality rate [8]. Moreover, some drugs usually taken by elderly people disturb the
339 normal perspiration or other processes that adjust body temperature, thereby

exacerbating the CVD mortality rate.

Elevated temperature during the summer caused by UHI is usually accompanied by increased air pollution, which yields a severe impact on CVDs. Atmospheric particulates triggered by heat waves increase in density, and increase the blood viscosity, pressure, and heart rate variability, thereby triggering diseases such as acute myocardial infarction [31]. Moreover, the increase in ozone density caused by high temperature exacerbates the CVD mortality. Some studies have proven that with every 10 $\mu g \cdot m^{-3}$ rise in ozone levels in the air, the CVD mortality rate among the Chinese population increases by 0.448% [32]. This is because the increased ozone density triggers inflammation, oxidative stress, and myocardial cell damage, and affects vessel structure and the transcription mechanism, lipid metabolism, and cardiovascular autonomic regulation [33].

Discussion

Our findings showed that UHIs have a significant effect on CVDs mortality by increasing ambient temperature in summer. Previous studies have proven that high temperatures are significantly correlated with CVDs mortality [34]. Baaghideh and Mayvaneh proposed that maximum air temperature was significantly positively correlated to CVDs mortality ($r = 0.83$, $p = 0.01$). The mortality rate increased by 4.27% per unit rise in maximum air temperature (95% confidence interval, 0.91–7.00) [35]. This is consistent with our study. And related studies have explained the reasons. heat waves activated the inflammation system, destroyed the structure of endothelial

cells in coronary arteries, increased the permeability of the tunica intima, reduced the superoxide dismutase activity of heart tissues, and finally increased the lipoprotein levels in oxygenated blood. As a result, high levels of cholesterol penetrated and were deposited on the tunica intima, causing atherosclerosis and exacerbating coronary heart disease [36].

Our findings revealed that the UHIs effect on CVDs have typical spatial and temporal characteristics. And the affected areas gradually expand to suburbs, mainly in central and southern urban areas. Previous studies have reported that high temperature clusters of heat wave in Beijing are mainly within the second ring road of Beijing, whereas heat wave risk obviously decreases from the second to sixth ring roads [37]. The spatial distribution of high temperature heat waves has certain similarities with our study, which further supports the impact of UHIs effect on CVDs. Meanwhile, the findings of this study demonstrated that the effect of UHI on CVDs evolves through three stages, namely concentric ring growth, axis expansion, and regional filling (Fig. 7).

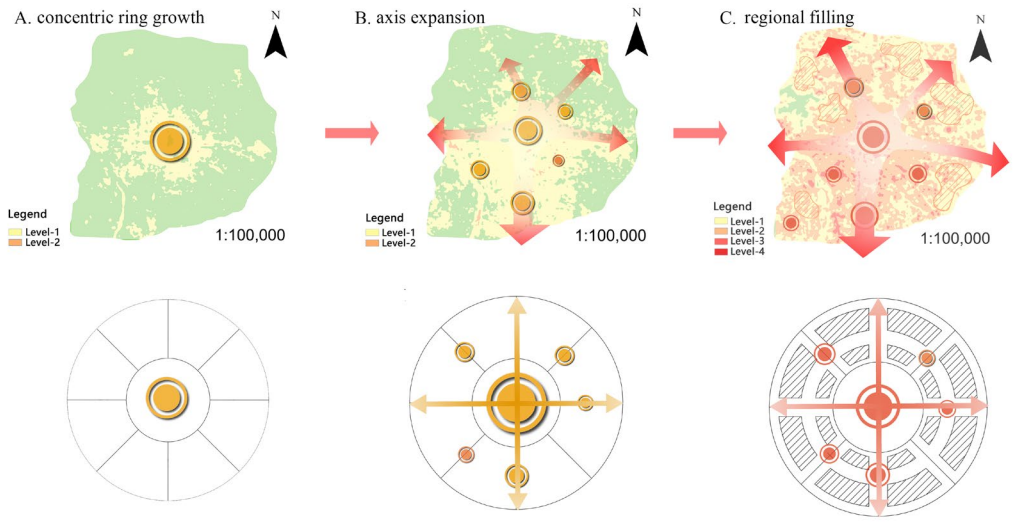

Fig. 7. Stages of form evolution of UHI on CVDs

We also found that UHIs have a typical landscape pattern process for the effect on CVDs. The overall landscape is distributed in a scattered manner. Similar studies revealed that the incidence of vector-borne Lyme disease is significantly related to the degree of regional landscape fragmentation and temperature [14]. Therefore, it is feasible to use the landscape pattern index method to study the effect of UHI on CVDs. This study provides a theoretical basis for the optimization of urban spatial structure and green space system. In the process of rapid urban development, according to the law of coordinated changes in environment and residents' health, the heat hazard sensitive space of the heat island is pre-judged, and then the countermeasures for the controllable and adjusted planning factors are taken.

This study had some limitations. One limitation is that we used the linear regression model; this study subtracted the effect of the intercept during air temperature retrieval to better reflect the intensity of UHI, resulting in overall underestimation of the effect on CVDs mortality. Finally, given the impact that weather and climate have on satellite images, this study used the two images to explore the spatio-temporal effect of UHI on CVDs during 1999–2017. The temperature-mortality relationship in this study cites the results of the Jinan study. The original study lacked data and did not consider air pollution, smoking, eating habits, etc., which may affect the temporal and spatial evolution of CVDs in UHI.

Conclusions

As UHI keeps intensifying, the effect level and area on CVDs show an upward trend and three evolution stages (concentric ring growth, axis expansion, and regional filling). The affected areas spread from the central urban area to suburbs, whereas more severely affected areas are mostly located in the central and southern areas.

The landscape pattern of the effect of UHI on CVDs reveals, in terms of quantity, a gradual fragmentation of the patches with the rise of patch quantity and density, and high-level patch plaque dominance. In terms of shape, the patches become irregular and space imbalanced; in terms of structure, the patch types of the entire landscape are more, yet weakly interconnected, whereas low-level areas are better interconnected in clusters.

UHI increases the environmental temperature during summer, and long-term exposure to high temperatures affects the functions of the human heart, thereby triggering CVDs and increasing the mortality rate during summer.

This study uses the landscape indices to assess the characteristics of the effect of UHI on CVDs, demonstrates the trend of spatio-temporal evolution of this effect, and provides theoretical evidence for early warning on CVDs.

List of abbreviations

AI, aggregation index; AREA_MN, mean patch area; CONTAG, contagion index; CVDs, cardiovascular diseases; ED, edge density; ICD-10, International Classification of Diseases, 10th revision; LSI, landscape shape index; LST, land surface temperature; NDVI, normalized difference vegetation index; NDWI,

normalized difference water index; NSAT, near-surface air temperature; PD, patch density; SHAPE_AM, shape index; SHDI, Shannon diversity index; UHI, urban heat island

Ethics approval and consent to participate: Not applicable.

Consent for publication: Not applicable.

Availability of data and materials:

The dataset is available from the corresponding author upon request.

Competing interests: The authors declare that they have no competing interests.

Funding:

This research was funded by the National Natural Science Foundation of China project (grant numbers 31971717 and 31600571) and the Top-notch Academic Programs Project of Jiangsu (grant number PPZY2015A063).

Authors' contributions:

HHC performed the data analyses and developed the study protocol. DX contributed significantly to analysis and refined the manuscript. YHL revised the manuscript. HC helped perform the analysis with constructive discussions. PZR played an important role in interpreting the results. LW performed the typesetting. All authors commented on the manuscript at various stages. All authors read and approved the final version of the paper.

Acknowledgements:

This study was supported by Professor Yun Yingxia.

References

1. United Nations. 68% of the world population projected to live in urban areas by 2050, says UN. 2018. Available from: https://www.un.org/development/desa/en/news/population/2018-revision-of-world-urbanization-prospects.html.
2. Baccini M, Biggeri A, Accetta G, Kosatsky T, Katsouyanni K, Analitis A, et al. Heat effects on mortality in 15 European cities. Epidemiology. 2008; 19:711–9.10.1097/EDE.0b013e318176bfcd.
3. World Health Organization. Cardiovascular diseases (CVDs). 2017. Available from: https://www.who.int/news-room/fact-sheets/detail/cardiovascular-diseases-(cvds).
4. Ostro BD, Roth LA, Green RS, Basu R. Estimating the mortality effect of the July 2006 California heat wave. Environ Res. 2009; 109:614–9. http://dx.doi.org/10.1016/j.envres.2009.03.010.
5. Kenney WL, Craighead DH, Alexander LM. Heat waves aging and human cardiovascular health. Med Sci Sports Exerc. 2014; 46:1891–9. https://doi.org/10.1249/MSS.0000000000000325.
6. Vandentorren S, Bretin P, Zeghnoun A, Mandereau-Bruno L, Croisier A, Cochet C, et al. August 2003 heat wave in France: Risk factors for death of elderly people living at home. Eur J Public Health. 2006; 16:583–91. https://doi.org/10.1093/eurpub/ckl063.
7. Silveira IH, Oliveira BFA, Cortes TR, Junger WL. The effect of ambie

nt temperature on cardiovascular mortality in 27 Brazilian cities. Sci T otal Environ. 2019; 691:996–1004. https://doi.org/10.1016/j.scitotenv.2019. 06.493.

8. Williams S, Nitschke M, Sullivan T, Tucker GR, Weinstein P, Pisaniell o DL, et al. Heat and health in Adelaide, South Australia: Assessment of heat thresholds and temperature relationships. Sci Total Environ. 20 12; 414:126–33. https://doi.org/10.1016/j.scitotenv.2011.11.038.
9. Wu, C.G., Cui, H.L., Lin, Y.Y., Wang, Y.W., Gong, Y.X., Ma, X.Y., 20 15. Analysis of the seasonal variation of urban heat island landscape p attern in Western Shenzhen based on Landsat TM data. Environ. Sci. T echnol. 38, 182-188. 10.3969/j.issn.1003-6504.2015.07.034(in Chinese)
10. Zhou, T.T., Lian, L.S., Li, B.F., Ji, X.L., 2017. The change of spatial-t emporal characteristics of Qingdao urban heat island based on remote s ensing. J. Earth Environ. 8, 157-168. https://doi.org/10.7515/JEE2017020 08(in Chinese).
11. Wu J, Smithwick EAH. Landscape fragmentation as a risk factor for b uruli ulcer disease in Ghana. Am J Trop Med Hyg. 2016; 95:63–9. htt ps://doi.org/10.4269/ajtmh.15-0647.
12. Liu H, Weng Q. An examination of the effect of landscape pattern, la nd surface temperature, and socioeconomic conditions on WNV dissemi nation in Chicago. Environ Monit Assess. 2009; 159:143–61. https://doi. org/10.1007/s10661-008-0618-6.

13. Tran PM, Waller L. Effects of landscape fragmentation and climate on lyme disease incidence in the Northeastern United States. Ecohealth. 2013; 10:394–404. https://doi.org/10.1007/s10393-013-0890-y.
14. Li J, Xu X, Yang J, Liu Z, Xu L, Gao J, et al. Ambient high temperature and mortality in Jinan, China: A study of heat thresholds and vulnerable populations. Environ Res. 2017; 156:657–64. http://dx.doi.org/10.1016/j.envres.2017.04.020
15. Zanter K. LANDSAT 8 (L8) DATA USERS HANDBOOK Version 1.0 June 2015. United States Geol Surv. 2015; 1:1–106.
16. Li N, Xu YM, He M, Wu XH. Retrieval of Apparent Temperaturein Beijing Based on Remote Sensing. Ecol Env.2018;27:1113-1121. https://doi.org/10.16258/j.cnki.1674-5906.2018.06.016(in Chinese).
17. Martin P, Baudouin Y, Gachon P. An alternative method to characterize the surface urban heat island. Int J Biometeorol. 2015; 59:849–61. https://doi.org/10.1007/s00484-014-0902-9.
18. Qin Z, Li W, Xu B, Jia L. The estimation of land surface emissivity for landsat TM6. Remote Sens L Resour. 2004;28-32. https://doi.org/10.3969/j.issn.1001-070X.2004.03.007 (in Chinese).
19. Liang YQ, Hong X, Xu F. Impacts of meteorological factors on death caused by cardiovascular disease in Nanjing City. Chinese J. Dis. Control Prev. 2015; 19: 24-27. https://doi.org/10.16462/j.cnki.zhjbkz.2015.01.001(in Chinese)

513 20. Chung JY, Honda Y, Hong YC, Pan XC, Guo YL, Kim H. Ambient t
514 emperature and mortality: An international study in four capital cities o
515 f East Asia. Sci Total Environ. 2009; 408:390–6. http://dx.doi.org/10.10
516 16/j.scitotenv.2009.09.009
517 21. Kang N, Li Z, Luo L, Ni H, Wu Y. Meteorological Assessment of Ec
518 ological Qualities and Bio-Meteorological Indicators in Ya'an. Plateau
519 Mt Meteorol Res. 2010; 30:36–42. 10.3969/j.issn.1674-2184·2010.03.006
520 (in Chinese).
521 22. Wang Y, Shen Y. Shanghai summer temperature and humidity effect an
522 d human comfort. J East China Norm Univ Sci. 1998;60–6. (in Chines
523 e).
524 23. Guo L, Xue D, Du S. Landscape ecological spatial pattern: planning a
525 nd evaluation. first. Beijing (in Chinese): China Environmental Science
526 Press; 2009. (in Chinese).
527 24. Huang J, Zhao X, Tang L, Qiu Q. Analysis on spatiotemporal changes
528 of urban thermal landscape pattern in the context of urbanization: A c
529 ase study of Xiamen City. Acta Ecol Sin. 2012; 32:0622–31. https://doi.
530 org/10.5846/stxb201012071745(in Chinese).
531 25. Qiao Z, Tian G, Zhang L, Xu X. Influences of urban expansion on ur
532 ban heat island in Beijing during 1989-2010. Adv Meteorol. 2014;2014.
533 https://doi.org/10.1155/2014/187169.
534 26. Madaniyazi L, Zhou Y, Li S, Williams G, Jaakkola JJK, Liang X, et a

l. Outdoor Temperature, Heart Rate and Blood Pressure in Chinese Adults: Effect Modification by Individual Characteristics. Sci Rep. 2016; 6: 1–9. http://dx.doi.org/10.1038/srep21003.

27. Zhang H, Wang Q, Zhang Y, Yang Y, Zhao Y, Sang J, et al. Modeling the impacts of ambient temperatures on cardiovascular mortality in Yinchuan: evidence from a northwestern city of China. Environ Sci Pollut Res. Environmental Science and Pollution Research; 2018; 25:6036–43. https://doi.org/10.1007/s11356-017-0920-3.

28. Basu R, Ostro BD. A multicounty analysis identifying the populations vulnerable to mortality associated with high ambient temperature in California. Am J Epidemiol. 2008; 168:632–7. https://doi.org/10.1093/aje/kwn170.

29. Cheng X, Su H. Effects of climatic temperature stress on cardiovascular diseases. Eur J Intern Med. European Federation of Internal Medicine; 2010; 21:164–7. https://doi.org/10.1016/j.ejim.2010.03.001.

30. Urban A, Davídkovová H, Kyselý J, Heat- and cold-stress effects on cardiovascular mortality and morbidity among urban and rural populations in the Czech Republic. Int. J. Biometeorol. 2014; 58: 1057-1068. https://doi.org/10.1007/s00484-013-0693-4.

31. Li G, Zhou M, Cai Y, Zhang Y, Pan X. Does temperature enhance acute mortality effects of ambient particle pollution in Tianjin City, China. Sci Total Environ. 2011; 409:1811–7. http://dx.doi.org/10.1016/j.scitot

env.2011.02.005.

32. Dong J, Liu X, Zhang B, Wang J, Shang K. Meta-analysis of associati on between short-term ozone exposure and population mortality in Chin a. Acta Sci Circumstantiae. 2016; 36:1477–85. https://doi.org/10.13671/j. hjkxxb.2015.0555 (in Chinese).
33. Yang H, Xi Z, Liu X, Chu N. Research Progress in Effects of Ozone on Cardiovascular System. 2018;2–5. https://doi.org/10.13704/j.cnki.jyyx. 2018.02.034(in Chinese).
34. Yang C, Meng X, Chen R, Cai J, Zhao Z, Wan Y, et al. Long-term v ariations in the association between ambient temperature and daily card iovascular mortality in Shanghai, China. Sci Total Environ. 2015; 538:5 24–30. http://dx.doi.org/10.1016/j.scitotenv.2015.08.097.
35. Baaghideh M, Mayvaneh F. Climate Change and Simulation of Cardiov ascular Disease Mortality: A Case Study of Mashhad, Iran. Iran J Publ ic Health. 2017; 46:396–407.
36. Zhang S, Zhang X, Tian Y, Wang B. Effect and its Mechanism of Art ificial Heat Wave on Coronary Heart Diseases. Meteorol Mon. 2015; 4 1:761–70. 10. 7519/j.issn.1000-0526.2015.06.011(in Chinese).
37. Xie GD, Zhang B, Lu CX, Xiao Y, Liu CL, Zhang B, et al. Rapid expansion of the metropolitan areas and impacts of resources and the environment. Resour. Sci. 2015; 37:1108-1114(in Chinese).

579

Figures

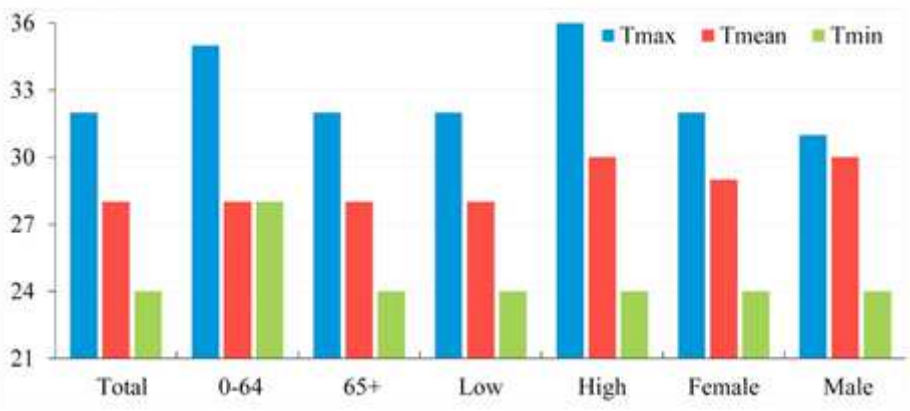

Figure 1

Heat thresholds of Tmax/Tmean/Tmin [14]

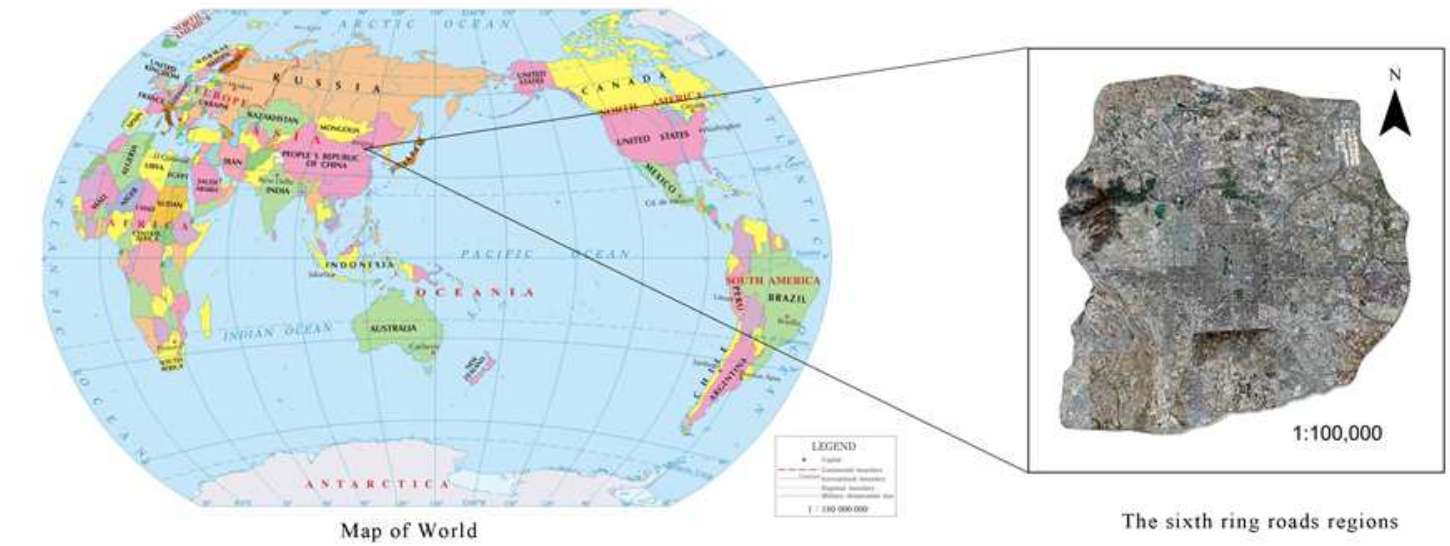

Figure 2

Outline of the study area Note: The designations employed and the presentation of the material on this map do not imply the expression of any opinion whatsoever on the part of Research Square concerning the legal status of any country, territory, city or area or of its authorities, or concerning the delimitation of its frontiers or boundaries. This map has been provided by the authors.

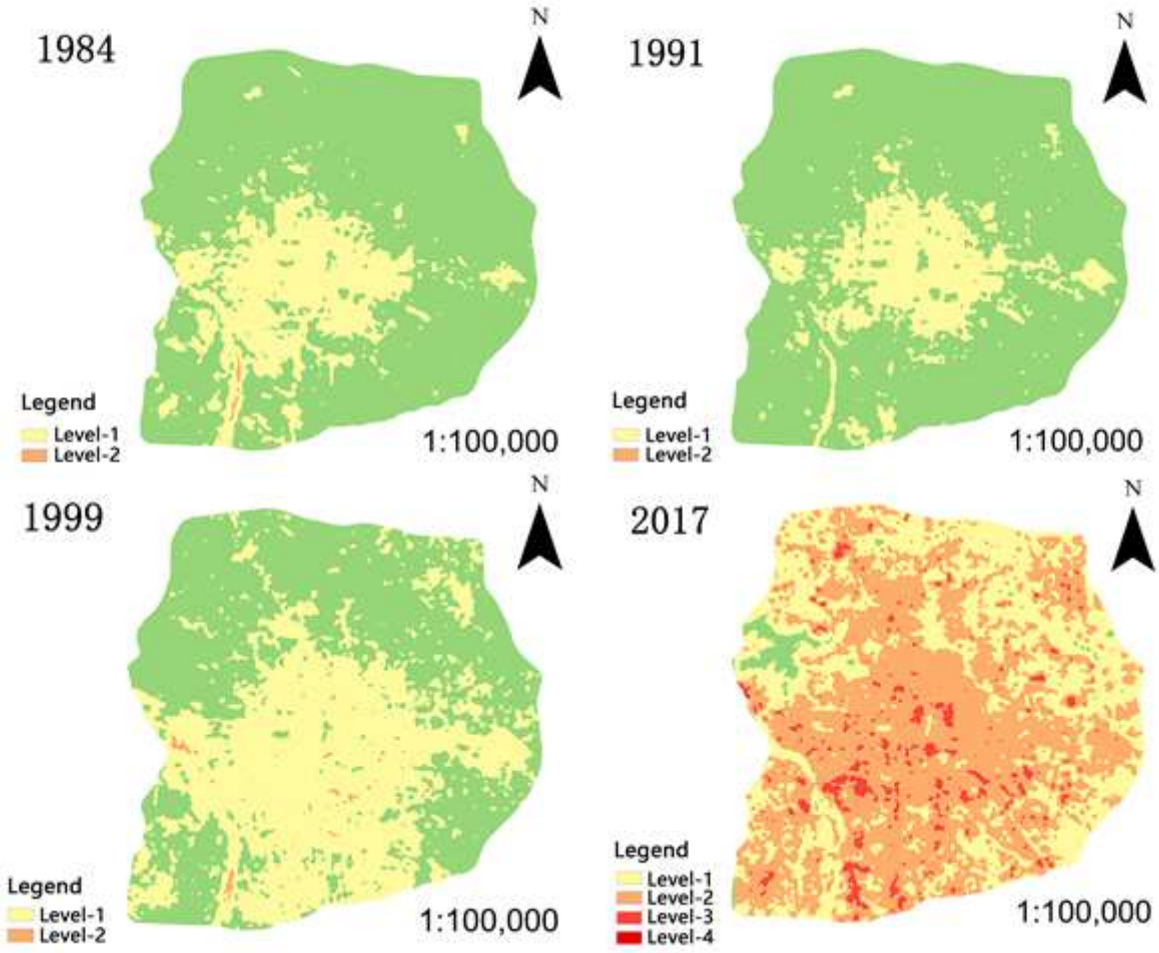

Figure 3

Distribution of affected areas during 1984–2017

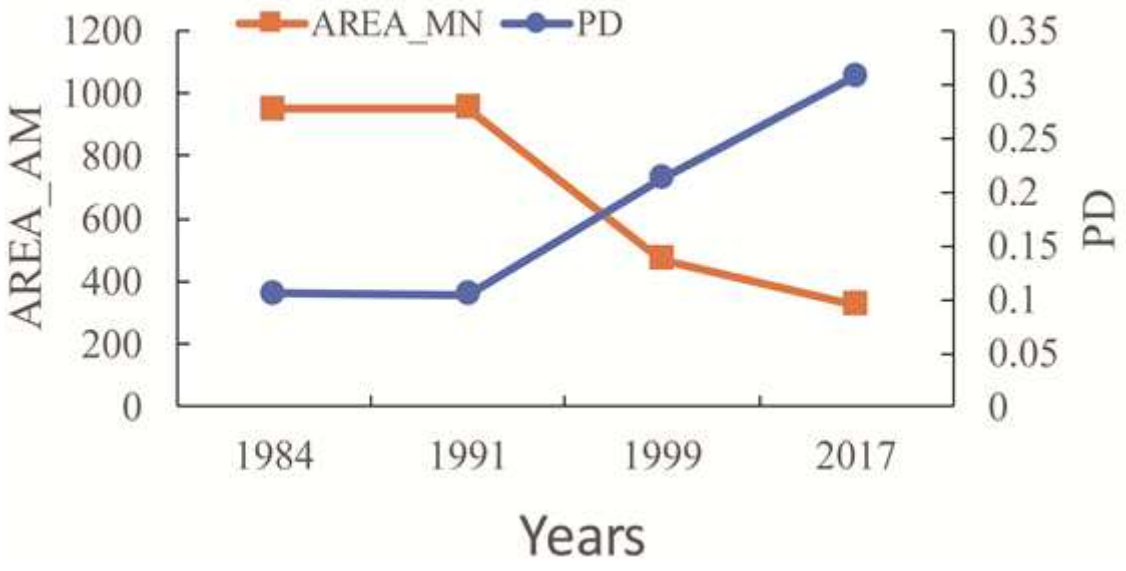

Figure 4

Changes in PD and AREA_MN during 1984–2017

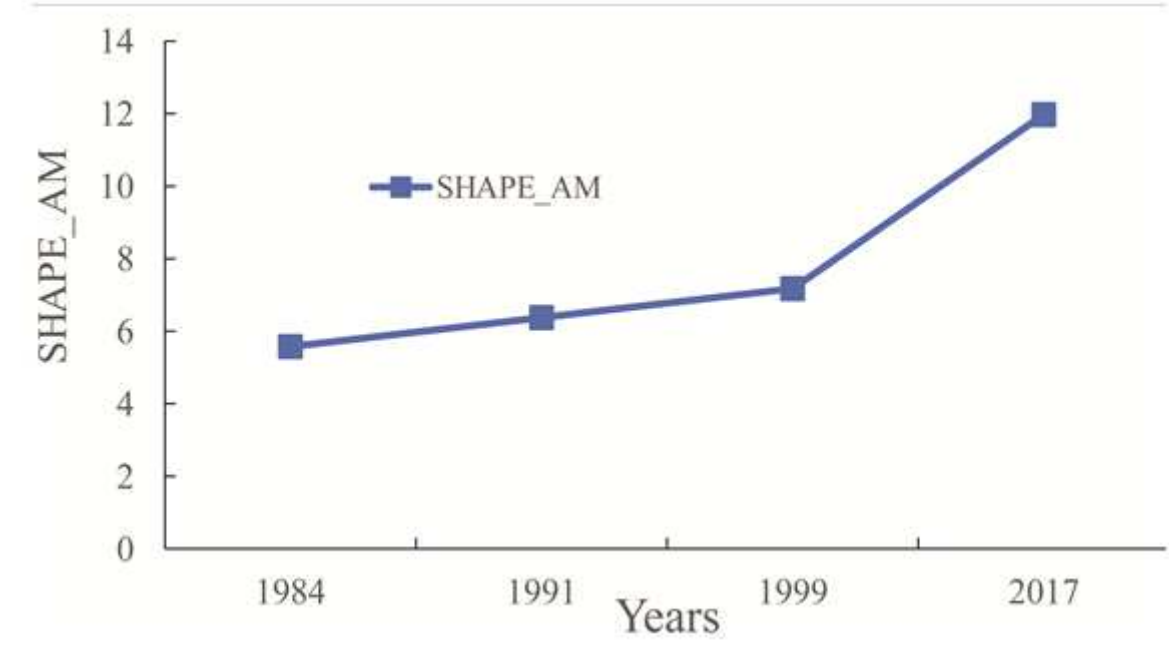

Figure 5

Changes in SHAPE_AM during 1984–2017

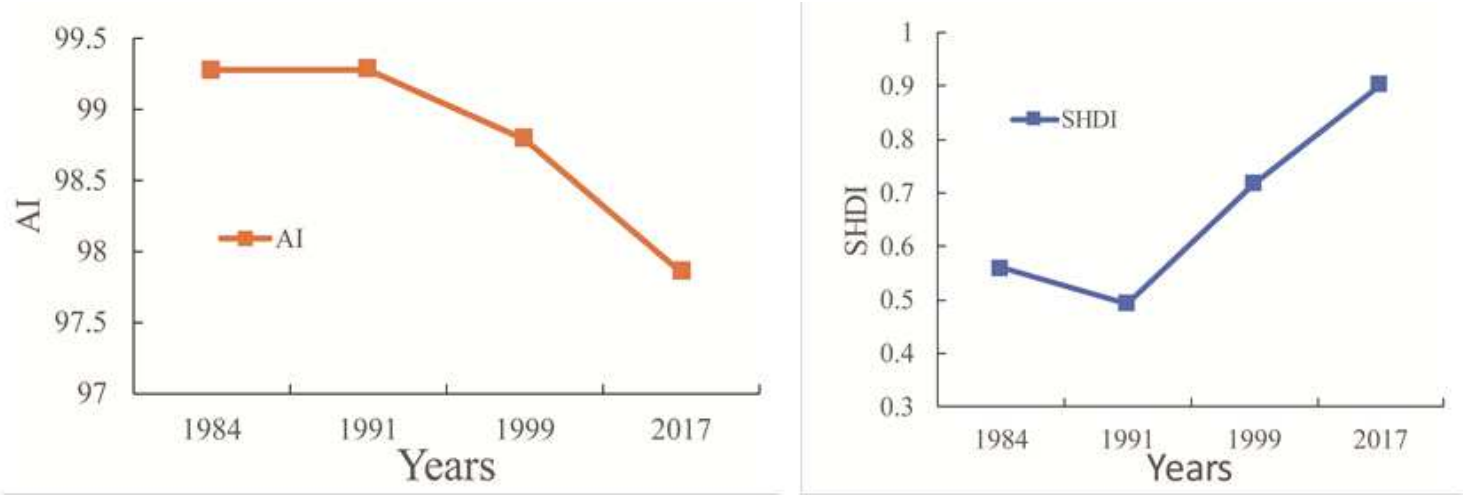

Figure 6

Changes in AI and SHDI during 1984–2017

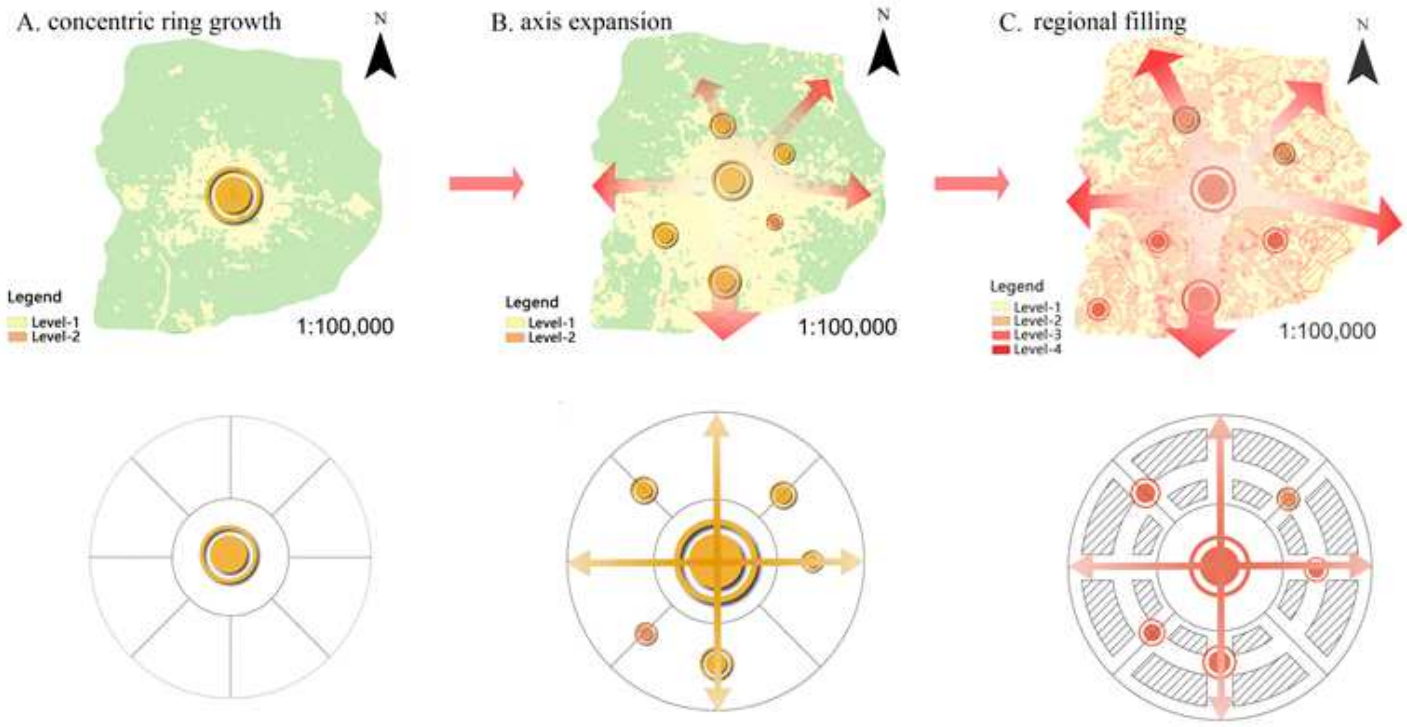

Figure 7

Stages of form evolution of UHI on CVDs